

Effects of Action Potential Duration on the Electrocardiogram in Type II Diabetes

R. Martin Arthur, Yujing Lin, Shuli Wang and Jason W. Trobaugh

Department of Electrical and Systems Engineering, Washington University School of Engineering
St. Louis, MO 63130

Correspondence: R. M. Arthur, Department of Electrical and Systems Engineering, Washington University in St. Louis
St. Louis, MO 63130. Email: rma@ese.wustl.edu

Abstract. Both diabetes and obesity cause cardiac dysfunction. To separate consequences of geometric changes with obesity from electrophysiological ones, we previously investigated how changes in cardiac and torso geometry affected body-surface electrocardiograms (ECGs). For this study, we characterized the sensitivity of body-surface potentials to diabetes-related AP changes by modeling normal cardiac-surface action potentials (APs) and prolonged APs, as seen in diabetic animal studies. We calculated ECGs using our bidomain model in a realistic heart and torso model. ECGs were characterized by changes in their iso-potential maps, standard 12-lead sets, and via temporal, spectral and principal component analysis. Relative differences over the body-surface during the T wave of 36, 93, and 157% were seen for AP duration increases of 29, 25, and 16 % in the base of the left ventricle (LV), apex of the LV, and the whole right ventricle, respectively. Simulation results were compared to measured values in normal and obese diabetic subjects. QT interval dispersion was underestimated in the precordial leads in the diabetic simulation and measurement by 20 and 94 msec, respectively. These results demonstrate both the sensitivity of the ECG to changes in the AP and the limitations of using standard lead sets to characterize electrocardiographic changes in diabetic subjects. They suggest the need for more comprehensive measures, such as body-surface mapping and inverse electrocardiography, to describe electrical remodeling due to diabetes.

Keywords: Action Potential Model, Body-surface Maps, Diabetes, Bidomain forward problem, Long QT, Heart-Torso models, 12-lead ECGs

1. Introduction

Myocardial disease is common in type II diabetes mellitus (T2DM). T2DM is accompanied by elevated risk for myocardial infarction, heart failure, and sudden cardiac death¹. Risk is monotonically increased with obesity, as measured, for example, by body-mass index (BMI)². Both diabetes and obesity are responsible for deleterious electrophysiological changes to the heart and for habitus changes to the heart and torso that affect body-surface electrocardiographic potentials (ECGs)^{3,4}. Previously we investigated effects on ECGs of body habitus changes induced by obesity⁵. Habitus changes may modify ECGs in ways that mask or confound changes due to diabetes. Here we examine the sensitivity of the ECG to changes in cardiac sources that may occur in diabetes to determine how useful surface measurements may be in assessing risk for T2DM.

Many studies have employed the standard 12-lead ECG to find risk indicators for cardiac dysfunction, cardiovascular disease, and all-cause mortality among T2DM patients^{1,6-13}. Changes in standard 12-lead ECGs with obesity and diabetes have been associated with ST segment depression, changes in QT intervals, T-wave morphology, and heart-rate variability^{1,9-12,14-16}. A primary risk correlate is the QT interval and its dispersion, that is, the difference between maximum and minimum QT values⁹⁻¹². Other changes may be important, but the full prognostic value of ECG abnormalities in

T2DM has probably not been realized, given the spatial sampling limits and vulnerability to habitus changes of 12-lead ECGs.

Our studies of risk for 1) ventricular tachycardia in post myocardial-infarction patients and 2) cardiac dysfunction in T2DM have highlighted the limitations of standard lead systems for assessing risk and for finding underlying markers of cardiac dysfunction for these and presumably other pathologies^{5,17-21}. To assess the electrical characteristics of cardiac dysfunction more fully than 12-lead analyses, we examined body-surface electrocardiographic maps to identify electrical phenotypes of cardiac dysfunction.

Certain pathological aspects of the diabetic heart have been found to be common to both human and animal models, including electrocardiographic changes such as prolongation of the QRS complex and the QT interval^{11,22}. Here, because of the limited availability of animal data for T2DM, we simulated the human diabetic heart based on the cardiac-surface action potential (AP) pattern found in a study on streptozotocin-induced Type 1 diabetic rats²³.

APs result from differences between intra- and extra-cellular potentials. Changes have been found in the ion channel currents across myocyte membranes in several diabetic animal studies²³⁻²⁷. Results suggest that, in diabetic rats, ion currents I_{to} , I_{ss} , and I_{Kr} are reduced during repolarization, which leads to prolonged AP duration (APD). In this study, we used AP changes during repolarization of cardiac-surface myocytes to characterize electrical remodeling that might be due to diabetes.

Based on results from diabetic animals, diabetic APs in humans were simulated by prolonging the duration of normal APs constructed using timing parameters exported from the software package ECGSIM²⁸. From simulated normal and diabetic APs over the cardiac surface, we calculated the corresponding normal and diabetic ECGs with our bidomain forward-problem platform^{5,29}. By computing differences between diabetic ECGs and normal ECGs over the whole torso, we explored the sensitivity of body-surface distributions to presumed diabetic electrical remodeling. Results drawn from these simulations were compared to measurements made on one normal and one obese T2DM subject.

2. Methods: Simulation and Measurement of Electrocardiograms in Humans

To study effects of changes in action potentials (APs) on electrocardiograms (ECGs), we simulated body-surface potentials with our bidomain forward-problem solution, whose derivation and validation have been reported previously^{5,29}. We also measured body-surface ECG maps in one normal and one obese diabetic subject for comparison to our simulations.

2.1 Electrocardiographic Response to Action Potential Changes

Our bidomain, forward-problem platform was used to calculate the effects of heart-torso geometry in order to find body-surface potentials, V , from cardiac-surface APs, Φ_m ^{5,29}. The bidomain forward-problem solution for the heart-torso model, A , yields V via matrix multiplication²⁹,

$$V = A\Phi_m \quad (1)$$

The ECGSIM package provided normal torso geometry and the timing of depolarization and repolarization that characterized cardiac-surface APs, but not AP shape²⁸. We used fixed templates for depolarization and repolarization waveforms. In this study those templates were based on logistic curves designed to match templates we used previously to study effects of obesity on body-surface potentials in T2DM. The previous templates used an arctangent function for depolarization and the dominant T wave for repolarization^{5,29,30}.

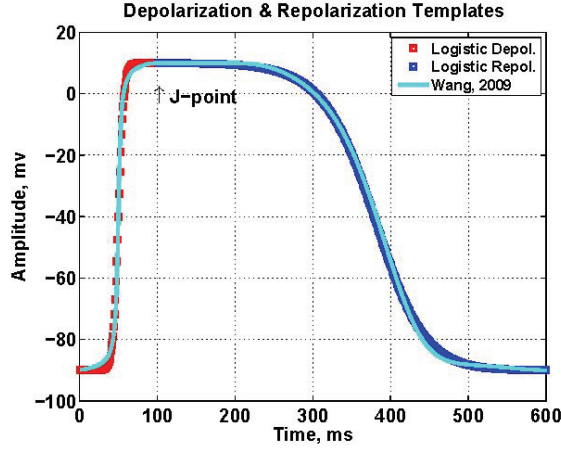


Fig. 1. Depolarization and repolarization templates based on logistic curves derived in this study compared to templates derived by Wang using an arctangent function for depolarization and the ECGSIM dominant T wave for repolarization^{5,28,29}.

Simulated Action Potentials using Logistic Curves: We found the action potentials, Φ_m , using logistic curves³¹, as defined in Eq. 3 below, the APs, in millivolts, are

$$\Phi_m(t, \Delta_{dep}, \Delta_{rep}) = 100\phi_{dep}(t, \Delta_{dep})\phi_{rep}(t, \Delta_{rep}) - 90 \quad , \quad (2)$$

where the depolarization waveform $\phi_{dep}(t, \Delta_{dep})$ at time t and at the heart-surface location where the maximal slope of the waveform occurs at time Δ_{dep} is

$$\phi_{dep}(t, \Delta_{dep}) = \frac{1}{[1+\exp(-a_1)(t-\Delta_{dep})]} \quad . \quad (3)$$

Similarly using $\Gamma_{rep}(t, \Delta_{rep})$, as a convenient intermediate expression given by

$$\Gamma_{rep}(t, \Delta_{rep}) = \int_0^t \frac{1}{[1+\exp(-a_2(\tau-\Delta_{rep}))]} \frac{1}{[1+\exp(a_3(\tau-\Delta_{rep}))]} d\tau \quad , \quad (4)$$

the repolarization waveform is

$$\phi_{rep}(t, \Delta_{rep}) = 1 - \Gamma_{rep}(t, \Delta_{rep})/\Gamma_{rep}(\infty, \Delta_{rep}) \quad . \quad (5)$$

The constants in these expressions were $a_1=0.30$, $a_2=0.0897-2.91 \times 10^{-4}$, $\gamma = 0.027$, $a_3=0.0255+4.31 \times 10^{-5}$, $\gamma = 0.035$. The activation recovery interval, γ , was set to 215.

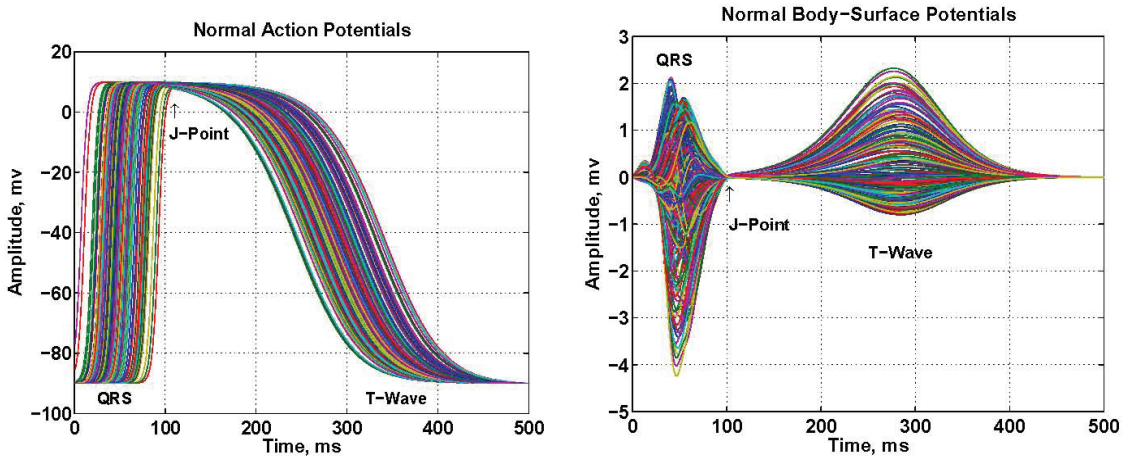


Fig. 2. Left) Action potentials calculated using Eq. 2 over the heart surface at the locations shown in Fig. 3 for a normal subject. Right) Body-surface potentials with respect to a central terminal calculated from the APs in the left panel using our bidomain forward-problem solution in the ECGSIM torso.^{5,28,29}

Figure 1 compares depolarization and repolarization AP templates, based on the logistic curves of Eqs. 3 and 5, to the templates used by Wang to match the shape of ECGSIM APs^{5,28,29}. Figure 2 shows

the logistic-templates used in Eq. 2 to calculate APs with normal values for Δ_{dep} and Δ_{rep} from ECGSIM²⁸. The APs in Figure 2, based on logistic-curves, were used in Eq. 1 to calculate normal body-surface potentials V , also shown in Fig. 2.

Simulated Long QT in Diabetes: Our framework for calculating APs and resultant ECGs allows us to investigate changes in ECGs caused by changes in the timing of depolarization and repolarization at each site on the heart surface. In this study we assessed effects on ECGs during the T wave due to alterations in the duration of cardiac-surface APs, in this case, to changes in Δ_{rep} .

To determine the sensitivity of ECGs to APD changes that might be found in diabetes we used data from the literature on diabetic rats. Among diabetic rats, action potential duration (APD) increase differed in three regions of the ventricle²³. The three regions were: 1) total right ventricle (RV), 2) subepicardium at the apex of the left ventricle (EpiALV), and 3) subendocardium at the base (EndoBLV). These regions are shown on the ventricular model exported from ECGSIM in Figure 3. APD in the rat, measured after 90% of repolarization (APD₉₀) had occurred, was prolonged by 80, 125 and 148% in the RV, EpiALV, and EndoBLV, respectively.

To apply the findings in diabetic rats to a human study, we multiplied the APD changes in the rat by a heart-rate correction factor. This factor used the normal pulse rates of the human and rat. According to American Heart Association, a normal human heart resting rate is 60 ~ 80 times a minute (bpm)³². Data from Yale Animal Resources Center indicate normal heart rate for a rat ranges 330 ~ 480 bpm³³. Using 360 and 72 bpm for rat and human heart rates, respectively, our correction factor was 0.2.

The resulting 16, 25 and 29% changes were used as APD prolongation percentages for the RV, EpiALV and EndoBLV areas of a human ventricle, respectively, to generate the diabetic APs used in our simulation studies. Body surface ECGs were calculated from both normal and diabetic APs in the same normal torso model for comparison.

2.2 Measurements in Normal & Obese Diabetic Subjects

Torso shape, ultrasonic images of the heart and electrocardiograms over the torso surface were measured in one normal subject and one obese diabetic patient. During acquisition of torso and heart geometry, subjects were immobilized with a Vac-LokTM (Civco Medical Solutions, Kalona, IA). Torso surface geometry and the location of 123 ECG electrode signals were measured with an Immersion 3D digitizer (Immersion Human Interface Corp., Palo Alto, CA). Heart size, orientation and location were determined with the images taken by a Terason 3000 ultrasonic imaging system (Teratech Corporation, Burlington, MA) with a 64-element, 2.5 MHz (4V2) linear array. A custom image-registration phantom was used to register ultrasonic images of the heart to the torso-surface geometry³⁴. Body-surface potentials were recorded with a 123-channel BioSemi mapping system (Amsterdam, Netherlands). Details of the experimental protocol have been reported previously^{5,29}.

The measured point cloud on the torso surface was used to form a 3D torso model using radial-basis functions with the Matlab FastRBFTM Toolbox from FarField Technology Limited (Christchurch, New Zealand). A heart model was digitized and used as a template. Based on the ultrasonic heart images, the template heart was shifted, rotated, scaled, and placed into the torso models³⁴. Heart and torso models along with the measured ECGs were used to solve conventional, boundary-element inverse problems^{35,36}. ECGs over the body-surface were calculated from these inverse solutions to produce maps at all locations in the torso model.

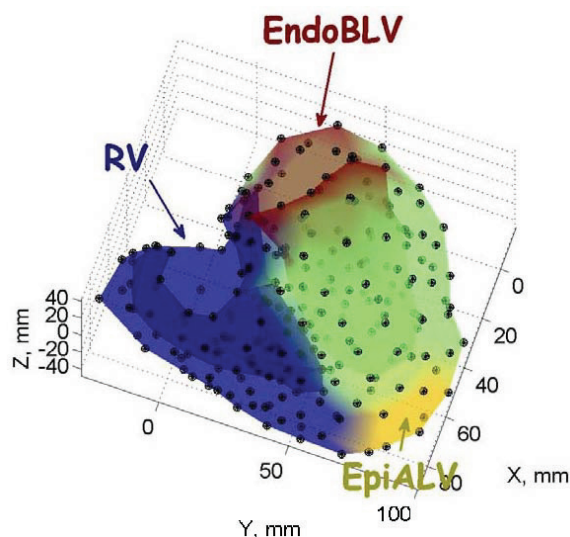


Fig. 3. ECGSIM²⁸ ventricle model with three regions in which APD increase was seen in the diabetic rat²³. Those regions were: 1) the whole wall of the right ventricle (RV) (in blue), 2) the subepicardium at the apex (EpiALV) (in yellow), and 3) the subendocardium at the base (EndoBLV) (in red). Black dots mark the 257 vertices of the triangular-element surface model.

2.3 Signal and Image Analysis

Body-surface potentials calculated due to AP changes were compared to normal values using iso-potential maps, standard 12-lead sets, and via temporal, spectral and principal component analysis. Body-surface potentials were reconstructed at all nodes on the torso models from inverse solutions in the normal and obese diabetic subjects for which the body-surface relative error was $< 5\%$ ³⁶.

We used iso-potential maps, which are ECG distributions on the body surface at a given instant during the cardiac cycle, to examine body-surface ECG patterns³⁷. To aid in classification, signals are often characterized by their spectra (frequency components)²⁰. Magnitudes of the Fourier transforms of ECGs over the T wave, averaged over the body surface for altered APs, were compared to ECG spectra due to normal APs. Principal component analysis (PCA) is another well-known data decomposition technique. It removes redundancy from body-surface ECGs^{38,39}, assuming that ECGs are a linear combination of orthogonal basis vectors. Principal components of body-surface ECGs during the T wave due to altered APs were compared to components of ECGs produced by normal APs.

Differences between normal ECGs and ones altered by APD changes were also characterized by relative difference (RD) and correlation coefficient (CC). RD, a measure of the amplitude differences, and CC, a measure of pattern similarity, are commonly used to evaluate forward and inverse electrocardiographic solutions⁴⁰. We used RD and CC to evaluate overall differences in body-surface ECGs at all torso sites during the T wave caused by regional changes in APs^{5,21,29}.

3. Results: Electrocardiographic Changes with Long QT in Diabetes

Diabetes has been associated with changes in ECGs^{11,22,23,27}. We evaluated those changes due to presumed diabetic electrical remodeling, represented as regional APD prolongation on the right ventricle, epi- and endo-cardial ventricular surfaces. ECGs were simulated from normal and presumed diabetic APs with our bidomain forward-problem solution using Eq. 1. Simulated results were compared to measurements in normal and obese diabetic subjects. We employed conventional signal processing tools to reveal spatial and temporal features of changes in ECGs from the diabetic during the QT interval and in particular over the T wave, as described in the Methods.

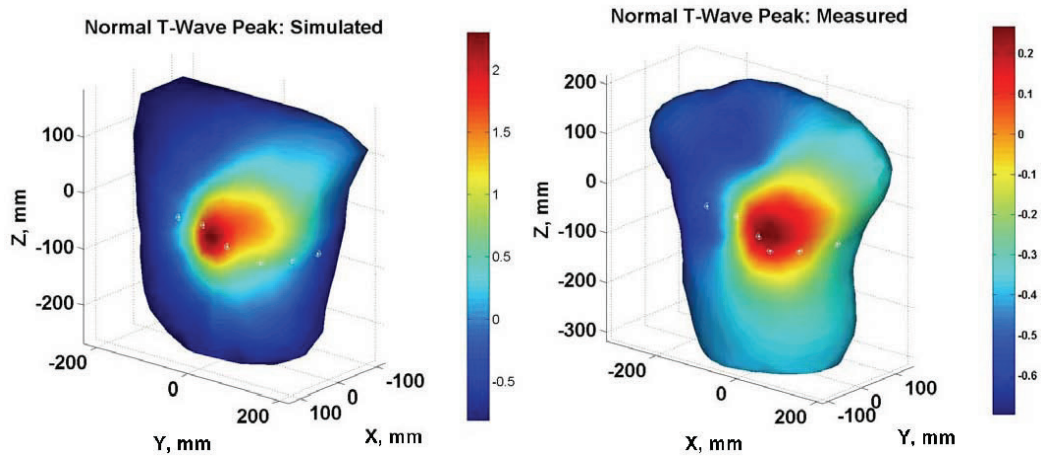


Fig. 4. Anterior body-surface, iso-potential maps at the peak of T wave. Left) Simulated map using the body-surface potentials shown in Fig. 2. Right) Measured map in a normal subject. The white dots mark the locations of precordial electrodes in the standard 12-lead system.

3.1 Iso-potential Maps

Comparison of iso-potential maps at a particular instant depicts the differences produced by changes in the APs that gave rise to those maps. Figure 4 shows the ECG potential distribution at the peak of the T wave for simulated and measured normal subjects. The peak of the T wave accounts for the largest energy measured on body surface during repolarization, which is presumed to be affected by the presence of diabetes. Note that the patterns for the simulated and measured distributions are similar.

Changes to the iso-potential patterns for regional changes in APs, depicted in Fig. 3, are shown in Figs. 5 and 6. Regional AP changes produce iso-potential patterns shown in Fig. 5 that are markedly different for the RV and ALV AP changes compared to the normal pattern, whereas the BLV pattern is similar to the normal one. Fig. 6 shows the pattern due to the sum of all the simulated regional AP changes compared to the measured pattern on an obese diabetic subject. Although the simulated and measured patterns differ, the main change in both simulated and measured patterns compared to normal is a shift in the positive peak toward the left shoulder.

To quantify these comparisons, we calculated the relative difference (RD) in maps produced by the altered APs compared to those produced by normal APs over the T wave. Those results are given in Table I. The RDs are large for all cases and the correlation is not strong except for the BLV AP changes. These results suggest that body-surface ECGs are likely to be sensitive to changes in AP duration that may be much smaller than those used in this study.

TABLE I
COMPARISON OF DIABETIC TO NORMAL ECGs OVER THE T WAVE AND THE BODY-SURFACE

	Diabetic	RV	ALV	BLV
Relative Difference, %	135.	157.	92.9	35.8
Correlation Coef.	0.42	0.38	0.64	0.98

3.2 Standard 12-Lead ECGs

In addition to body-surface ECGs, the standard 12-lead set was also employed because of its prevalence in clinical diagnosis. In the 12-lead set, only eight signals are independent. Here we compared the six precordial leads (V1-V6), as shown in Fig. 7. Dramatic changes occurred in 12-lead ECGs due to the APD prolongation associated with diabetes. As expected, an obvious delay of the T wave was seen because of the AP prolongation. In addition, compared with normal, precordial lead measurements were inverted in leads V2, V3 and V4. Whether or not these changes or others in the precordial leads are of diagnostic value is not clear, particularly given the habitus change with obesity that often accompanies T2DM and may dramatically alter the geometric relationship between the heart

and the precordial electrode locations⁵.

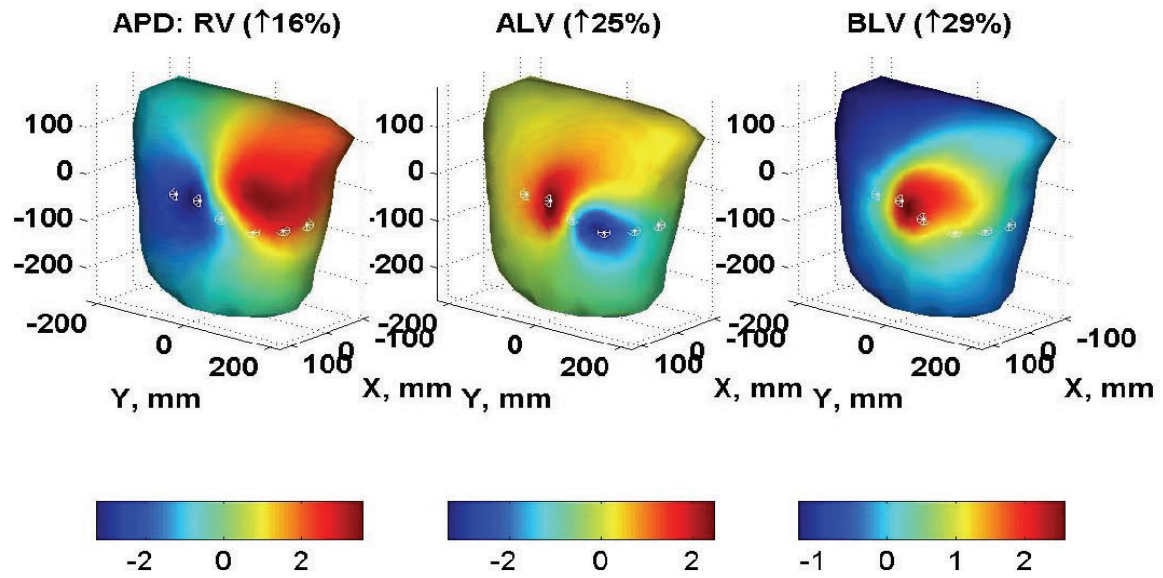


Fig. 5. Variation of anterior body-surface potential maps in the ECGSIM torso²⁸ at the peak of the T wave with regional AP duration (APD) increases (see Fig. 3). Left) APD was increased in the right ventricle by 16% compared to normal. Center) APD increased in the subepicardium at the apex by 25%. Right) APD increased in the subendocardium at the base of the left ventricle by 29%. The white dots in all three maps mark the locations of precordial electrodes in the standard 12-lead system.

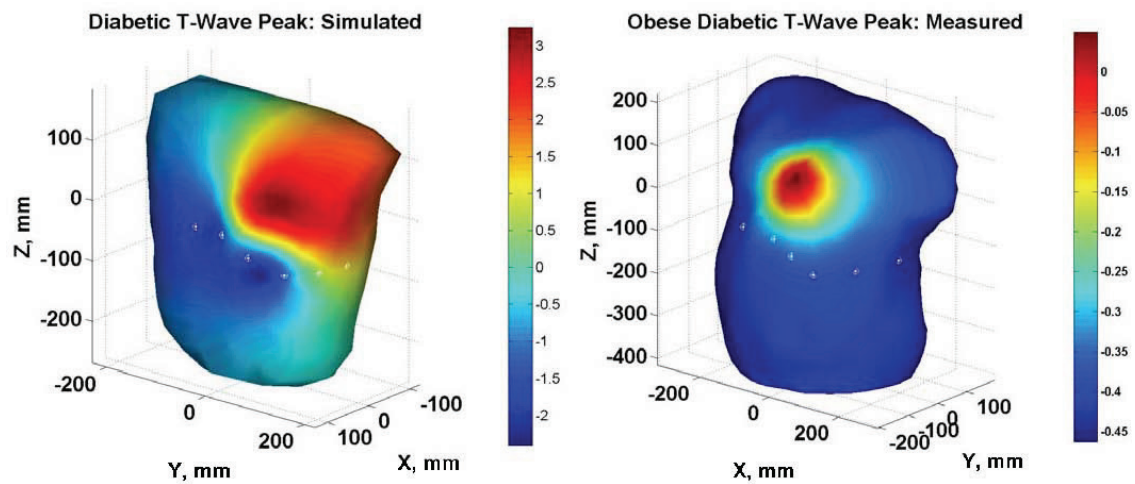


Fig. 6. Anterior body-surface, iso-potential maps at the peak of T wave. Left) Simulated map using body-surface potentials calculated from APs that combined all of the regional increases shown in Fig. 5. Right) Measured map in an obese diabetic subject. The white dots mark the locations of precordial electrodes in the standard 12-lead system.

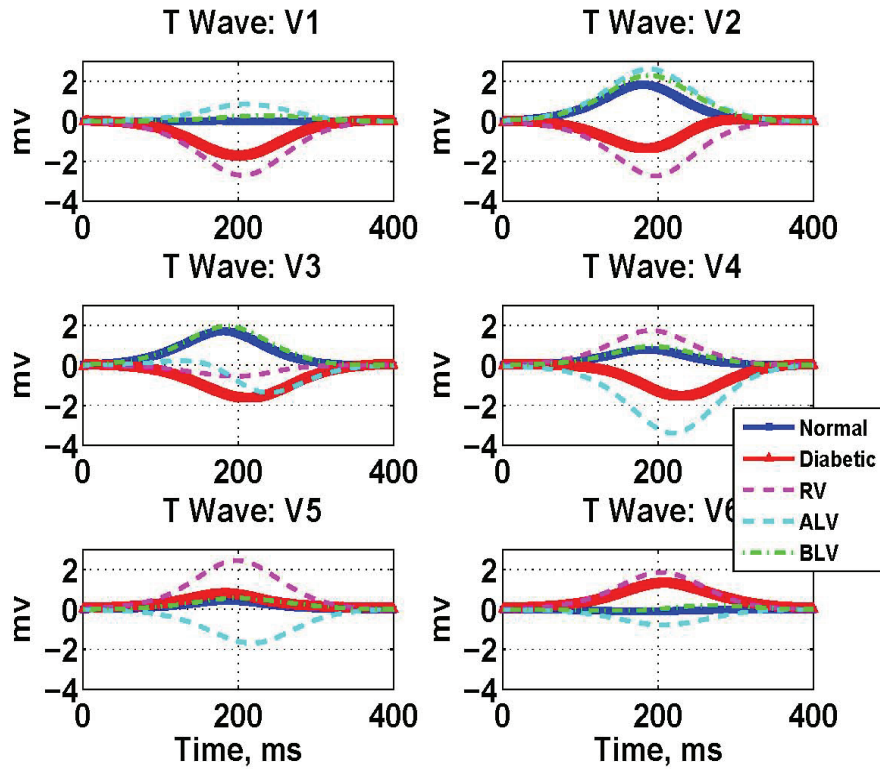


Fig. 7. Simulated precordial ECGs from the standard 12-lead set during the T wave in a normal subject and in a diabetic subject with regional changes in APD seen in animal studies, as described in Fig. 5. See Figs. 4 and 6 for the locations of the precordial electrodes and the corresponding iso-potential maps at the peak of the T wave due to normal and diabetic APs.

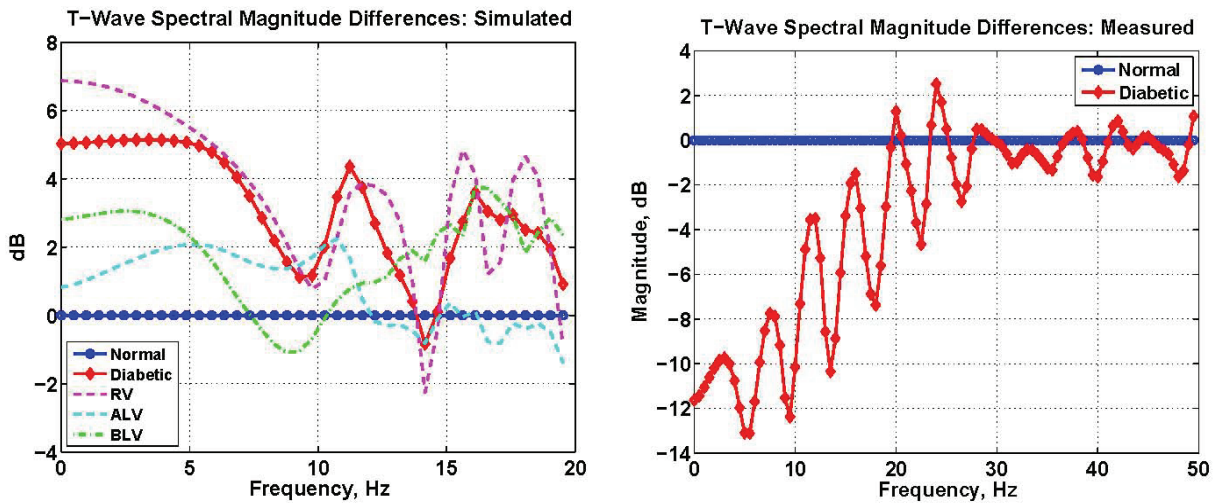


Fig. 8. Spectral magnitude differences during the T wave in body-surface ECGs. The spectral magnitude from the normal subject was set to 0 dB at each frequency and the other spectra adjusted accordingly. Left) Simulated differences from ECGs due to diabetic APs (see Figs. 5 and 6) relative to spectra from ECGs generated with normal APs. Right) Measured differences in one diabetic subject relative to measurements in one normal subject.

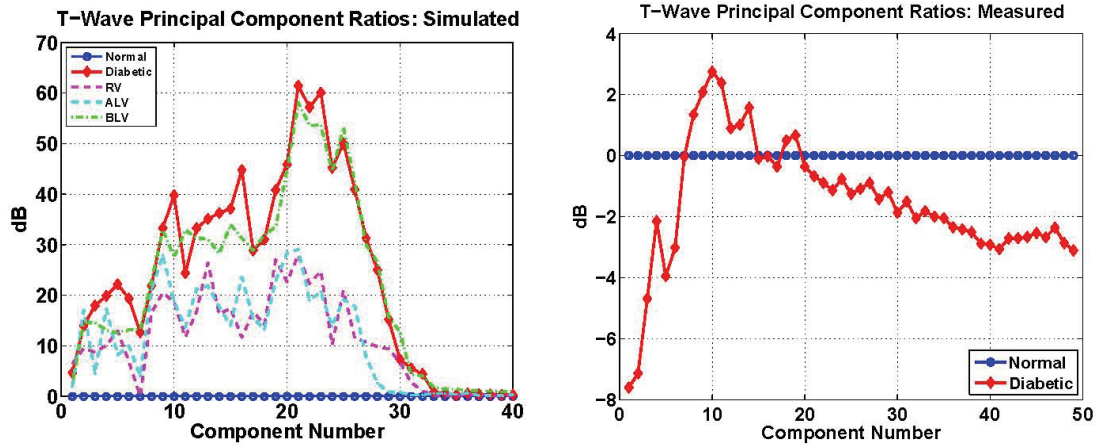


Fig. 9. Principal component ratios during the T wave in body-surface ECGs. Each principal component magnitude from the normal subject was set to 0 dB and the other component values adjusted accordingly. Left) Simulated ratios from ECGs due to diabetic APs (see Figs. 5 and 6) relative to components from ECGs generated with normal APs. Right) Measured ratios in one diabetic subject compared to measurements in one normal subject.

3.3 Spectral and Principal Component Analyses

To capture the harmonic content of the body-surface energy distribution, spectrum analysis was used to determine the spectral magnitudes of the Fourier transforms of both simulated and measured ECGs. Means of the spectral magnitudes during the T wave from diabetic ECGs were compared to spectra from normal ECGs as shown in Fig. 8. At each frequency the magnitudes were adjusted so that normal was always at 0 dB¹⁷. Results suggest that the prolongation of APD caused an increase in the strength of the low-frequency components of the ECGs. The measured result shows the opposite effect: the low frequency components are smaller. Principal components from both simulated and measured ECGs are compared in Fig. 9. APD increase in the simulations is associated with an increase in component strength, but the measured PCA ratios do not agree, particularly for the first few components. Results in the next section may help explain the differences between the simulations and the measurements.

3.4 Spatial Standard Deviation

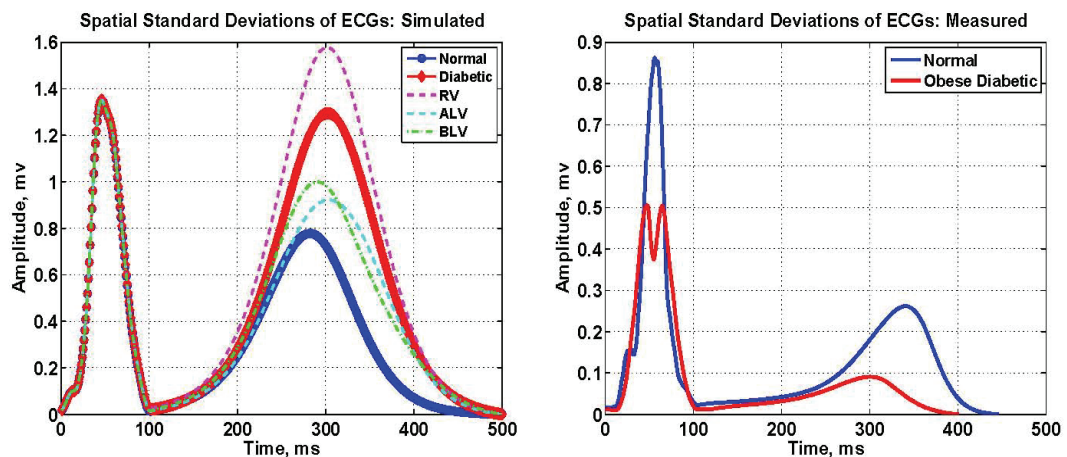
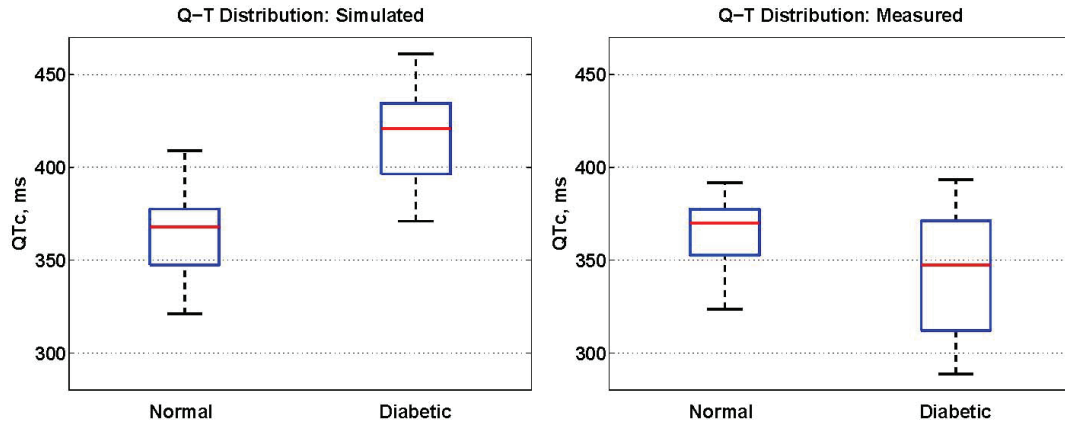


Fig. 10. Standard Deviations of ECGs over the body surface during the QT interval. Left) Simulated values from normal ECGs and from ECGs due to diabetic APs (see Figs. 5 and 6). Right) Measured values from one diabetic subject and one normal subject.

Spatial standard deviations (SSDs) of ECGs were calculated for measured normal and diabetic subjects, as well as for simulated normal and diabetic ECGs, as shown in Fig. 10. They describe the

signal strength over the torso at each instant of time in the QT interval. In the simulations, SSD strength was increased for the regional prolongations in APD and for the sum of all APD increases. In contrast, the measured SSD strength for the diabetic subject was much smaller than that of the normal subject. Note that the smaller signal in the diabetic may be due to his obese habitus. Also note the measured difference in SSDs over the QRS complex in T2DM compared to normal. These differences



may be a marker of T2DM.

Fig. 11. Distribution of QTc (QT intervals corrected for heart rate) in normal and diabetic subjects. The boxes have lines at the lower quartile, median, and upper quartile values. The whiskers show the extent of the rest of the data. Left) Simulated QTc. Right) Measured QTc. For both simulations and measurements, differences between normal and diabetic QTc values were significant ($p < 0.0001$).

3.5 QT Intervals

Spectral, PCA and SSD measurements compared to simulation for prolonged AP duration suggest that, at least based on this study, QT prolongation may not be the major consequence of diabetes. Nevertheless, QT interval is an important ECG feature that has been investigated as an indicator for diabetes^{11,41,42}. Instead of using QT itself, we evaluated the corrected QT value (QTc) for both subjects. Here, the QTc was calculated from QT with a standard clinical correction for heart rate using Bazett's formula⁴³, $QTc = \frac{QT}{\sqrt{RR}}$, where RR is the interval between the peaks of successive R waves in seconds. Fig. 11 demonstrates the QTc distributions based on the ECGs of both the normal control and diabetic subjects from both simulations and measurements. The results indicate there is a significant difference in QTc between the normal and diabetic subjects in both the simulated and measured values, with $p < 0.0001$ in each case. In addition, QTd, or QT dispersion, the difference between the maximum and minimum QTc values may be of diagnostic value. QTd reflects the underlying heterogeneity of ventricular repolarization. In contrast to most clinical QT studies, we used body-surface ECGs in addition to the standard 12-lead ECGs to calculate the QTc and QTd. Table II summarizes the QTd results for simulations and measurements in normal and diabetic subjects. It also gives the underestimation of QTd when using the precordial leads alone compared to using measurements over the whole torso.

TABLE II
QTd (DISPERSION) IN MSEC
COMPARISON OF SIMULATED AND MEASURED NORMAL AND DIABETIC VALUES
DIFFERENCES BETWEEN BODY-SURFACE (BS) AND PRECORDIAL LEAD (PL) VALUES

	Normal			Diabetic		
	Body Surface	Precordial Leads	BS-PL	Body Surface	Precordial Leads	BS-PL
Simulated	88	82	6	90	70	20
Measured	68	23	45	105	11	94

4. Discussion and Conclusions

In this study, diabetic electrical remodeling was characterized as regional APD prolongation, described using logistic functions and based on findings in diabetic animal studies. Normal and diabetic ECGs were calculated with our bidomain forward-problem solution and compared to measurements in normal and diabetic subjects. Simulations showed that ECGs are sensitive to relatively small changes in AP duration as seen in the analyses of the ECG spectra and principal components. Interestingly, however, spectra and principal component changes in the simulations did not match measured values. In addition, although QT_c was prolonged in simulation, as expected for prolonged APs, it was not longer in our diabetic subject compared to QT_c in our normal subject. Nor was QRS extended in the diabetic subject (see Fig. 10), as has been observed by others^{11,22}.

These results suggest the animal model we used is not an appropriate match for our human study and that better animal models are needed for the study of the cardiac electrical consequences of diabetes⁴⁴. Another possibility is that QRS and QT prolongation had not developed in our diabetic subject, because he was diagnosed early in the progression of the disease. Obviously, one diabetic subject is not an adequate base from which to draw conclusions, but these results do call for further study.

Clinical data on the effects of T2DM on ECGs include changes in the QT interval⁹⁻¹². QT corrected for heart rate and QT dispersion, however, remain controversial measures because their clinical utility is unclear⁴⁵. Although both simulated and measured QT distributions differed significantly in this study ($p < 0.0001$), the measured diabetic QT_c median was less than that for the measured normal subject. His dispersion of QT was greater than that for the normal subject (105 versus 68 msec). Perhaps, more importantly, the measured value of 105 msec over the torso surface was 94 msec longer than that extracted from the precordial leads. The presumed inability to capture the full range of the QT values may be one factor that limits the clinical utility of QT measures based on the 12-lead set.

Both habitus changes with obesity and cardiac source changes with diabetes affect the ECG. This situation probably makes the problem of identifying the electrical phenotype of T2DM too complex for 12-lead analysis alone. The use of body-surface maps and inverse solutions to characterize cardiac source changes in T2DM may be needed to get a comprehensive, stable measure of the electrical condition of the heart in obese diabetic subjects with cardiac pathologies.

5. Acknowledgments

This work was supported in part by National Institute of Health grant R01-HL50295 and by the Wilkinson Trust at Washington University. We are grateful to Alan D. Waggoner, Research Associate Professor of Medicine, for his help in acquiring the ultrasonic images used in this study.

References

- [1] PM Okin, RB Devereux, ET Lee, JM Galloway, and BV Howard, "Electrocardiographic repolarization complexity and abnormality predict all-cause and cardiovascular mortality in diabetes.the strong heart study," *Diabetes*, vol. 53, pp. 434–440, February 2004.
- [2] WC Willett, WH Dietz, and GA Colditz, "Guidelines for healthy weight," *The New England Journal of Medicine*, vol. 341, no. 6, pp. 427–434, 1999.
- [3] RB Devereux, MJ Roman, M Paranicas, MJ O'Grady, ET Lee, TK Welty, RR Fabsitz, D Robbins, ER Rhoades, and BV Howard, "Impact of diabetes on cardiac structure and function. the strong heart study," *Circulation*, vol. 101, pp. 2271–2276, 2000.
- [4] SM Grundy, B Howard, S Smith, Jr, R Eckel, R Redberg, and RO Bonow, "Prevention conference VI: Diabetes and cardiovascular disease: Executive summary: Conference proceeding for healthcare professionals from a special writing group of the american heart association," *Circulation*, vol. 105, pp. 2231–2239, 2002.
- [5] RM Arthur, S Wang, and JW Trobaugh, "Changes in body-surface electrocardiograms from geometric remodeling with obesity," *IEEE Trans on Biomed Engr*, vol. 58, no. 6, pp. 1565–1573, 2011.
- [6] PM Okin, RB Devereux, BV Howard, RR Fabsitz, ET Lee, and TK Welty, "Assessment of qt interval and qt dispersion for prediction of all-cause and cardiovascular mortality in American indians: The strong heart study," *Circulation*, vol. 101, pp. 61–66, 2000.
- [7] BV Howard, ET Lee, LD Cowan, RB Devereux, JM Galloway, OT Go, WJ Howard, ER Rhoades, DC Robbins, ML Sievers, and TK Welty, "Rising tide of cardiovascular disease in American indians the strong heart study," *Circulation*, vol. 99, pp. 2389–2395, 1999.
- [8] SM Grundy, A Garber, R Goldberg, S Havas, R Holman, C Lamendola, WJ Howard, P Savage, J Sowers, and GL Vega, "Prevention conference vi: Diabetes and cardiovascular disease: Writing group iv: Lifestyle and medical management of risk factors," *Circulation*, vol. 105, pp. 165–169, 2002.
- [9] AAO Naas, NC Davidson, C Thompson, F Cummings, SA Ogston, RT Tung, RW Newton, and AD Struthers, "QT and QTc

- dispersion are accurate predictors of cardiac death in newly diagnosed non-insulin dependent diabetes: Cohort study," *Br Med J*, vol. 316, pp. 745–746, 1998.
- [10] PT Sawicki, S Kiwitt, R Bender, and M Berger, "The value of QT interval dispersion for identification of total mortality risk in non-insulin dependent diabetes mellitus," *J of Internal Med*, vol. 243, pp. 49–56, 1998.
 - [11] PK Christensen, MA Gall, A Major-Pedersen, A Sato, P Rossing, L Breum, A Pietersen, J Kastrup, and HH Parving, "QTc interval length and QT dispersion as predictors of mortality in patients with noninsulin-dependent diabetes," *Scand J Clin Lab Invest*, vol. 60, pp. 323–332, 2000.
 - [12] M Veglio, M Borra, LK Stevens, JH Fuller, and PC Perin, "The relation between QTc interval prolongation and diabetic complications. the EURODIAB IDDM complication study group," *Diabetologia*, vol. 42, pp. 68–75, 1999.
 - [13] QZ Liu, WC Knowler, RG Nelson, MF Saad, MA Charles, IM Liebow, PH Bennett, and DJ Pettitt, "Insulin treatment, endogenous insulin concentration, and eeg abnormalities in diabetic pima indians: cross-sectional and prospective analyses," *Diabetes*, vol. 41, no. 9, pp. 1141–1150, 1992.
 - [14] H-C Chiu, A Kovacs, RM Blanton, X Han, M Courtois, CJ Weinheimer, KA Yamada, S Brunet, H Xu, JM Nerbonne, MJ Welch, NM Fettig, TL Sharp, N Sambandam, KM Olson, DS Ory, and JE Schaffer, "Transgenic expression of fatty acid transport protein 1 in the heart causes lipotoxic cardiomyopathy," *Circ Res*, vol. 96, pp. 225–233, 2005.
 - [15] T Lindstrom, L Jorfeldt, L Tegler, and HJ Arqvist, "Hypoglycaemia and cardiac arrhythmias in patients with Type 2 diabetes mellitus," *Diabetic Med*, vol. 9, no. 6, pp. 536–41, 1992.
 - [16] G Molon, G Targher, A Costa, L Bertolini, E Barbieri, and L Zenari, "Measurement of microvolt T-wave alternans, a new arrhythmic risk stratification test, in Type 2 diabetic patients without clinical cardiovascular disease," *Diabetic Med*, vol. 23, pp. 207–210, 2006.
 - [17] ME Cain, HD Ambos, J Markham, BD Lindsay, and RM Arthur, "Diagnostic implications of spectral and temporal analysis of the entire cardiac cycle in patients with ventricular tachycardia," *Circulation*, vol. 83, pp. 1637–1648, 1991.
 - [18] NG Kavesh, ME Cain, HD Ambos, and RM Arthur, "Enhanced detection of distinguishing features in signal-averaged electrocardiograms from patients with ventricular tachycardia by combined spatial and spectral analyses of entire cardiac cycle," *Circulation*, vol. 90, no. 1, pp. 254–263, 1994.
 - [19] RM Arthur, NG Kavesh, HD Ambos, and ME Cain, "Phase and group-delay characteristics of signal-averaged electrocardiograms from patients with ventricular tachycardia," *IEEE Trans on Biomed Engr*, vol. 42, no. 1, pp. 29–41, 1995.
 - [20] ME Cain, RM Arthur, and JW Trobaugh, "Detection of the fingerprint of the electrophysiological abnormalities that increase vulnerability to life-threatening ventricular arrhythmias," *J of Intervent Cardiac Electrophys*, vol. 9, pp. 103–118, 2003.
 - [21] RM Arthur, S Wang, and JW Trobaugh, "Changes in body-surface electrocardiograms from geometric remodeling due to obesity," *IntJ of Bioelectromagnetism*, vol. 11, no. 1, pp. 46–49, 2009.
 - [22] P Rossing, L Breum, A Major-Pedersen, A Sato, H Winding, A Pietersen, J Kastrup, and HH Parving, "Prolonged qtc interval predicts mortality in patients with type 1 diabetes mellitus," *Diab Med*, vol. 18, pp. 199–205, 2001.
 - [23] O Casis, M Gallego, M Iriarte, and JA Sanchez-Chapula, "Effects of diabetic cardiomyopathy on regional electrophysiologic characteristics of rat ventricle," *Diabetologia*, vol. 43, pp. 101–109, 2000.
 - [24] A Nishiyama, DB Ishii, PH Backx, BE Pulford, BR Birks, and MM Tamkun, "Altered K⁺ channel gene expression in diabetic ventricle: isoform switching between Kv4.2 and Kv1.4," *Am J Physiol. Heart CircPhysiol*, vol. 281, pp. H1800–H1807, 2001.
 - [25] Z Xu and GJ Rozanski, "K⁺ current inhibition by amphiphilic fatty acid metabolites in rat ventricular myocytes," *Am J Physiol Cell Physiol*, vol. 275, pp. 1660–1667, 1998.
 - [26] NK Bracken, AJ Woodall, FC Howarth, and J Singh, "Voltage-dependence of contraction in streptozotocin-induced diabetic myocytes," *Molecular and Cell Biochem*, vol. 261, pp. 235–243, 2004.
 - [27] FC Howarth, M Jacobson, O Naseer, and E Adeghate, "Short-term effects of streptozotocin-induced diabetes on the electrocardiogram, physical activity and body temperature in rats," *Experimental Physiology*, vol. 90, no. 2, pp. 237–245, 2005.
 - [28] A van Oosterom and TF Oostendorp, "ECGSIM: an interactive tool for studying the genesis of QRST waveforms," *Heart*, vol. 90, pp. 165–168, 2004.
 - [29] S Wang, *Electrocardiographic Consequences of Electrical and Anatomical Remodeling in Diabetic and Obese Humans*, Ph.D. thesis, Department of Electrical and Systems Engineering, Washington University, St. Louis, MO, USA, 2009.
 - [30] A van Oosterom, "The dominant T wave and its significance," *J CardiovascElectrophysiol*, vol. 14, pp. S180–S187, 2003.
 - [31] A van Oosterom and V Jacquemet, "A parameterized description of transmembrane potentials used in forward and inverse procedures," *Folia Cardiologica*, vol. 12 (suppl. D), pp. 111–114, 2005.
 - [32] Johan E.P. Waktare, "Cardiology patient page -atrial fibrillation," *Circulation*, vol. 106, pp. 14–16, 2002.
 - [33] Yale University Yale Animal Resources Center, "Veterinary clinical services -normative data," [http : //www.med.yale.edu/yarc/vcs/normativ.htm](http://www.med.yale.edu/yarc/vcs/normativ.htm).
 - [34] JW Trobaugh and RM Arthur, "Methods for using ultrasound to generate a heart surface for electrocardiographic inverse problems," *Int J of Bioelectromagnetism*, vol. 5, pp. 314–315, 2003.
 - [35] RC Barr, M Ramsey, III, and MS Spach, "Relating epicardial to body surface potential distributions by means of transfer coefficients based on geometry measurements," *IEEE Trans on Biomed Engr*, vol. BME-24, pp. 1–11, 1977.
 - [36] DG Beetner and RM Arthur, "Estimation of heart-surface potentials using regularized multipole sources," *IEEE Trans on Biomed Engr*, vol. 51, pp. 1366–1373, 2004.
 - [37] DM Mirvis, "Current status of body surface electrocardiographic mapping," *Circulation*, vol. 75, pp. 684–688, 1987.
 - [38] K Evans, RL Lux, MJ Burgess, RF Wyatt, and JA Abildskov, "Redundancy reduction for improved display and analysis of body surface potential maps II Temporal compression," *Circ Res*, vol. 49, pp. 197–203, 1981.
 - [39] PM Okin, RB Devereux, E Gerdtz, SM Snapinn, KE Harris, S Jern, SE Kjeldsen, S Julius, JM Edelman, LH Lindholm, and B Dahlöf, "Impact of diabetes mellitus on regression of electrocardiographic left ventricular hypertrophy and the prediction

- of outcome during antihypertensive therapy. The Losartan Intervention for Endpoint (LIFE) Reduction in Hypertension Study” *Circulation*, vol. 113, pp. 1588–1596, 2006.
- [40] C Ramanathan, P Jia, R Ghanem, D Calvetti, and Y Rudy, “Noninvasive electrocardiographic imaging (ECGI): Application of the generalized minimal residual (gmres) method,” *Annals of Biomedical Engineering*, vol. 31, pp. 981–994, 2003.
- [41] GF Salles, W Deccache and CRL Cardoso, “Usefulness of qt-interval parameters for cardiovascular risk stratification in type 2 diabetic patients with arterial hypertension,” *J of Human Hypertension*, vol. 19, pp. 241–249, 2005.
- [42] M Psallasa, N Tentolourisa, D Papadogiannisa, D Doulgerakisa, A Kokkinosa, DV Cokkinosb, and N Katsilambros, “QT dispersion Comparison between participants with Type 1 and 2 diabetes and association with microalbuminuria in diabetes,” *J of Diabetes and Its Complications*, vol. 20, pp. 88–97, 2006.
- [43] HC Bazett, “An analysis of the time-relations of electrocardiograms,” *Heart*, vol. 7, pp. 353–370, 1920.
- [44] WT Cefalu, “Animal models of type 2 diabetes: Clinical presentation and pathophysiological relevance to the human condition,” *ILAR Journal*, vol. 47, no. 3, pp. 186–198, 2006.
- [45] BR Shah, T Yamazaki, G Engel, S Cho, SH Chun, and VF Froelicher, “Computerized QT dispersion measurement and cardiovascular mortality in male veterans,” *Am J Cardiol*, vol. 93, pp. 483–486, Feb 2004.